Organozinc Derivatives of Deltahedral Zintl Ions: Synthesis and Characterization of *closo*-$[E_9Zn(C_6H_5)]^{3-}$ (E = Si, Ge, Sn, Pb)

Jose M. Goicoechea and Slavi C. Sevov*

Department of Chemistry and Biochemistry, University of Notre Dame, Notre Dame, Indiana 46556

Received May 31, 2006

Reactions of group 14 deltahedral Zintl ions E_9^{4-} (E = Si, Ge, Sn, Pb) with diphenylzinc yielded the organically functionalized heteroatomic *closo*-clusters $[E_9Zn\text{-}Ph]^{3-}$ (E = Si (**1**), Ge (**2**), Sn (**3**), Pb (**4**)). All four clusters exhibit the same bicapped square antiprismatic geometry in which one of the capping positions is occupied by the ZnPh organometallic fragment. Three filled molecular orbitals of the cluster overlap with three empty orbitals at the ZnPh fragment, and the cluster acts as a six-electron ligand analogous to cyclopentadienyl and benzene ligands. The species were characterized by single-crystal X-ray diffraction in $[K(2,2,2\text{-crypt})]_3[Si_9Zn(C_6H_5)]\cdot 2py$, $[K(2,2,2\text{-crypt})]_3[Ge_9Zn(C_6H_5)]\cdot 2en\cdot tol$, $[K(2,2,2\text{-crypt})]_3[Sn_9Zn(C_6H_5)]\cdot tol$, and $[K(2,2,2\text{-crypt})]_6[Pb_9Zn(C_6H_5)]_2\cdot 2en\cdot tol$. The presence of these clusters in solution was confirmed by electrospray mass spectrometry and $^{13}C\{^1H\}$ NMR experiments.

Introduction

The chemistry of deltahedral Zintl clusters has witnessed somewhat of a renaissance in recent years as the reactivity of these anionic species toward a series of d^6 and d^{10} transition metal reagents has been explored. A wealth of novel clusters, many of which exhibit exciting new geometries, have been isolated by reaction of the aforementioned transition metal adducts with nine-atom Zintl ions of germanium, tin, and lead. As a result, two broad categories of transition metal derivatized Zintl clusters have been isolated. In the first instance are those clusters in which the nuclearity of the naked nine-atom Zintl ion is maintained and the clusters are centered and/or capped by transition metal fragments. Examples of these species are the ML_n capped clusters $[Ge_9Ni(CO)]^{3-}$ and $[E_9M(CO)_3]^{4-}$ (E = Sn, Pb; M = Cr, Mo, W)[1,2] and the transition metal centered and ML capped species $[Pt@Sn_9Pt(PPh_3)]^{2-}$,[3] $[Ni@Sn_9Ni(CO)]^{3-}$,[3] $[Ni@Ge_9NiL]^{2-}$ (L = CO, PPh_3),[1,4] and $[Ni@Ge_9NiL]^{3-}$ (L = en, C≡CPh).[1] All of these species were obtained by reactions between ethylenediamine solutions of the Zintl ions E_9^{4-} (E = Ge, Sn, Pb) and transition metal reagents with one or several labile ligands such as $Ni(COD)_2$ (COD = cyclooctadiene), $M(PPh_3)_4$ (M = Pd, Pt), $Ni(PPh_3)_2(CO)_2$, or $LM(CO)_3$ (M = Cr, Mo, W; L = mesitylene, cycloheptatriene, or toluene).

The second class of transition metal derivatized clusters differs in the number of main group atoms with regard to the original naked E_9 clusters. Examples are $[Ni@Pb_{10}]^{2-}$,[5] $[Pt@Pb_{12}]^{2-}$,[6] $[Ni_2Sn_{17}]^{4-}$,[7] $[Ni(Ni@Ge_9)_2]^{4-}$,[8] and $[Pd_2@Ge_{18}]^{4-}$.[9] In all of them, the transition metal centers the clusters and plays a crucial role in stabilizing these higher nuclearities and geometries that would be otherwise unattainable. Although the interstitial atoms do not bring additional electrons to the clusters as they are all closed-shell d^{10} atoms, they provide orbitals that can overlap with the cluster orbitals and stabilize the larger geometries from within. Most affected is the totally bonding molecular orbital made of the radial atomic orbitals of the cluster atoms. Without interstitial atoms the overlap between these radial contributions decreases as the diameter of the cluster increases, ultimately making these geometries unstable. Emtpy clusters of nine atoms appeared to be the upper limit until the recent discovery of Pb_{10}^{2-} proved this assumption wrong.[10]

In addition to the reactions of deltahedral Zintl anions with transition metal adducts, reactivity studies of Ge_9^{n-} (n = 2, 3, 4) clusters toward a series of main group anionic nucleophiles (Nu^-) such as Ph_2Sb^-, Ph_2Bi^-, Ph_3Ge^-, Ph_3Sn^-, and Me_3Sn^- have been carried out by our research group over the past several years.[11] As a result of these investigations, we have compiled a library of species with two-center−two-electron *exo*-bonds to the aforementioned nucleophiles, resulting in functionalized clusters such as $[Ge_9\text{−}R]^{3-}$, $[R\text{−}Ge_9\text{−}R]^{2-}$, and $[R\text{−}Ge_9\text{−}Ge_9\text{−}R]^{4-}$. To describe these derivatized species, we need to highlight first some important features in the geometry and charges of the naked nine-atom clusters. Their overall shape is based on a tricapped trigonal prism. Slight distortions in this geometry allow the clusters to accommodate three distinct charges of 2−, 3−, and 4−, i.e., E_9^{2-}, E_9^{3-}, and E_9^{4-}.[11c,12] The tricapped trigonal

* To whom correspondence should be addressed. E-mail: ssevov@nd.edu.

(1) Goicoechea, J. M.; Sevov, S. C. *J. Am. Chem. Soc.* **2006**, *128*, 4155.

(2) (a) Eichhorn B. W.; Haushalter, R. C.; Pennington, W. T. *J. Am. Chem. Soc*. **1988**, *110*, 8704. (b) Kesanli, B.; Fettinger, J.; Eichhorn, B. *Chem. Eur. J*. **2001**, *7*, 5277. (c) Eichhorn, B. W.; Haushalter, R. C. *Chem. Commun.* **1990**, 937. (d) Campbell, J.; Mercier, H. P. A.; Holger, F.; Santry, D.; Dixon, D. A.; Schrobilgen, G. J. *Inorg. Chem.* **2002**, *41*, 86. (e) Yong, L.; Hoffmann, S. D.; Fässler, T. F. *Eur. J. Inorg. Chem.* **2005**, 3663.

(3) Kesanli, B.; Fettinger, J.; Gardner, D. R.; Eichhorn, B. *J. Am. Chem. Soc.* **2002**, *124*, 4779.

(4) (a) Gardner, D. R.; Fettinger, J. C.; Eichhorn, B. W. *Angew. Chem., Int. Ed. Engl.* **1996**, *35*, 2852. (b) Esenturk, E. N.; Fettinger J.; Eichhorn B. *Polyhedron* **2006**, *25*, 521.

(5) Esenturk, E. N.; Fettinger, J.; Eichhorn, B. W. *Chem. Commun.* **2005**, 247.

(6) Esenturk, E. N.; Fettinger, J.; Lam, Y.-F.; Eichhorn, B. W. *Angew. Chem., Int. Ed.* **2004**, *43*, 2132.

(7) Esenturk, E. N.; Fettinger, J. C.; Eichhorn, B. W. *J. Am. Chem. Soc.* **2006**, *128*, 12.

(8) Goicoechea, J. M.; Sevov, S. C. *Angew. Chem., Int. Ed.* **2005**, *44*, 2.

(9) Goicoechea, J. M.; Sevov, S. C. *J. Am. Chem. Soc.* **2005**, *127*, 7676.

(10) Spiekermann, A.; Hoffmann, S. D.; Fässler, T. F. *Angew. Chem., Int. Ed.* **2006**, *45*, 3459.

(11) (a) Ugrinov, A.; Sevov, S. C. *J. Am. Chem. Soc.* **2002**, *124*, 2442. (b) Ugrinov, A.; Sevov, S. C. *J. Am. Chem. Soc.* **2003**, *125*, 14059. (c) Ugrinov, A.; Sevov, S. C. *Chem. Eur. J.* **2004**, *10*, 3727.

(12) For recent reviews on E_9^{n-} (n = 2−4) clusters see: (a) Corbett, J. D. *Chem. Rev.* **1985**, *85*, 383. (b) Corbett, J. D. *Struct. Bonding* **1997**, *87*, 157. (c) Corbett, J. D. *Angew. Chem., Int. Ed.* **2000**, *39*, 670. (d) Fässler, T. F. *Coord. Chem. Rev.* **2001**, *215*, 377.

10.1021/om060481g CCC: $33.50
Publication on Web 08/19/2006

prismatic shape associated with a *closo*-E_9^{2-} can be easily distorted by elongation of one, two, or all three of the prismatic edges parallel to the 3-fold axis, and the cluster adds one or two more electrons because a formerly empty molecular orbital is stabilized by the distortions. In the particular case of a single elongated edge, the cluster geometry resembles that of a monocapped square antiprism and is often more conveniently discussed as such. In all of the main group functionalized species, the *exo*-bonds with the R groups are at the vertexes of the elongated edges. The same bonding mode is also observed in Ge_9 oligomers such as $[Ge_9-Ge_9]^{6-}$,[13] $[Ge_9=Ge_9=Ge_9]^{6-}$,[14] and $[Ge_9=Ge_9=Ge_9=Ge_9]^{8-}$,[15] as well as in the polymers $_\infty[-(Ge_9)^{2-}-]$ and $_\infty[-(Hg-Ge_9)^{2-}-]$.[16,17] The clusters in the trimer and tetramer are bonded with two bonds along two elongated edges in each cluster and are no longer two-center−two-electron bonds.

There is clearly a disparity between the behavior of transition metal complexes and main group reagents with respect to the addition site at the nine-atom deltahedral clusters of group 14. In an attempt to bridge this divide, we explored the reactivity of these clusters with elements at the borderline between transition and main group metals such as those of group 12. The elements of this group are known to possess a certain duality, which allows them to behave as either transition or alkaline-earth metals. We recently reported the reaction of the organozinc compound $ZnPh_2$ with polyatomic bismuth anions that yielded the novel intermetalloid species $[Zn_9Bi_{11}]$.[5−18] Reported herein is the outcome of analogous reactions of $ZnPh_2$ with the nine-atom deltahedral clusters of group 14 that produced the ZnPh-substituted *closo*-clusters $[E_9Zn\text{-}Ph]^{3-}$ (E = Si (**1**), Ge (**2**), Sn (**3**), Pb (**4**)). The ZnPh fragment adds to the cluster at the same open-square position as the previously observed transition metal fragments $M(CO)_3$ (M = Cr, Mo, W) and Ni(CO).[1,2] This is the first complete series of clusters of group 14 functionalized with one and the same fragment. Furthermore, cluster **1** represents the first example of a functionalized Si_9 cluster, which further expands the field of Zintl cluster chemistry of silicon following the recent characterization of Si_9^{3-}, Si_9^{2-} and Si_5^{2-}.[19]

Results and Discussion

Synthesis. The four species reported herein were obtained by reactions of liquid ammonia or ethylenediamine solutions of the corresponding nine-atom deltahedral Zintl ions E_9^{4-} (E = Si, Ge, Sn, Pb) with stoichiometric amounts of diphenylzinc. Liquid ammonia was employed for the dissolution of the $K_{12}Si_{17}$ phase,[20] as it is not soluble in more common laboratory solvents, whereas ethylenediamine was used as a solvent for the remaining group 14 solid-state precursors K_4E_9 (E = Ge, Sn, Pb).[21,22] The $[K(2,2,2\text{-crypt})]^+$ (2,2,2-crypt = 4,7,13,16,21,24-hexaoxa-1,10-diazabicyclo[8.8.8]hexacosane) salts of clusters **2**−**4** were crystallized in high yields from ethylenediamine solutions layered with toluene. The silicon analogue, $[Si_9Zn$-

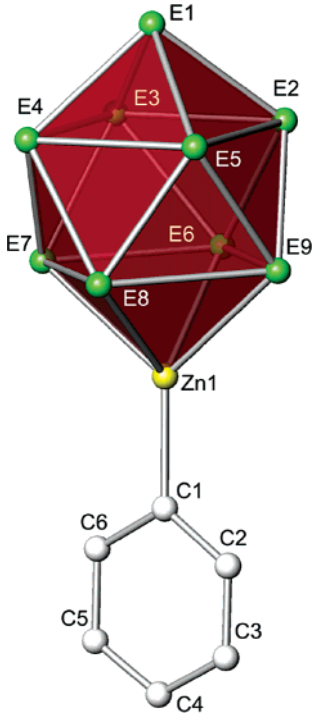

Figure 1. $[E_9Zn\text{-}Ph]^{3-}$ (E = Si, Ge, Sn, Pb): a 10-atom *closo*-deltahedron with the shape of a bicapped square antiprism where one of the capping atoms is the zinc atom of the ZnPh fragment.

Table 1. Bond Distances [Å] for the *closo*-Bicapped Square Antiprismatic Clusters 1−4

atoms[a]	1	2	3	4[b]
E1−E2	2.418(3)	2.5688(7)	2.9323(3)	3.0704(6), 3.0611(6)
E1−E3	2.419(3)	2.5565(7)	2.9344(3)	3.0447(6), 3.0482(5)
E1−E4	2.409(3)	2.5615(7)	2.9478(3)	3.0718(5), 3.0468(6)
E1−E5	2.419(3)	2.5683(8)	2.9471(3)	3.0698(5), 3.0743(6)
E2−E3	2.645(3)	2.8356(7)	3.2199(3)	3.4069(6), 3.3620(6)
E2−E5	2.666(3)	2.8377(8)	3.1422(3)	3.2915(5), 3.3273(6)
E2−E6	2.405(3)	2.5427(7)	2.9450(3)	3.0466(6), 3.0863(5)
E2−E9	2.399(3)	2.5499(8)	2.9412(3)	3.0700(5), 3.0597(6)
E3−E4	2.640(3)	2.8311(7)	3.2275(3)	3.4078(5), 3.3330(6)
E3−E6	2.405(3)	2.5469(7)	2.9375(3)	3.0800(6), 3.0635(6)
E3−E7	2.404(3)	2.5487(7)	2.9408(3)	3.0514(5), 3.0649(6)
E4−E5	2.689(3)	2.8132(8)	3.2067(3)	3.3050(6), 3.2897(5)
E4−E7	2.401(3)	2.5598(8)	2.9156(3)	3.0690(6), 3.0647(5)
E4−E8	2.400(3)	2.5483(8)	2.9165(3)	3.0715(6), 3.0717(6)
E5−E8	2.407(3)	2.5523(8)	2.9652(3)	3.1130(5), 3.0871(5)
E5−E9	2.395(3)	2.5597(8)	2.9577(3)	3.0711(6), 3.0695(5)
E6−E7	2.578(3)	2.7884(7)	3.1572(3)	3.3381(5), 3.3273(6)
E6−E9	2.612(3)	2.7883(8)	3.1028(3)	3.2607(5), 3.2989(5)
E7−E8	2.587(3)	2.7671(7)	3.1423(3)	3.2675(6), 3.2567(5)
E8−E9	2.611(3)	2.7722(8)	3.0926(3)	3.2071(5), 3.2716(6)
Zn1−E6	2.519(2)	2.5720(8)	2.7867(4)	2.8005(12), 2.8074(13)
Zn1−E7	2.504(2)	2.5944(9)	2.7397(4)	2.7883(13), 2.8114(13)
Zn1−E8	2.531(3)	2.5868(9)	2.7772(4)	2.8387(13), 2.8206(13)
Zn1−E9	2.518(3)	2.5889(9)	2.7799(4)	2.8411(12), 2.8268(12)
Zn1−Ph	2.000(9)	1.994(5)	1.987(3)	2.001(11), 1.983(10)

[a] Numbering of the atoms is shown in Figure 1. [b] There are two crystallographically distinct $[Pb_9Zn\text{-}Ph]^{3-}$ clusters in the asymmetric unit for $[K(2,2,2\text{-crypt})]_6[Pb_9Zn\text{-}Ph]_2\cdot 2en\cdot tol$.

(13) (a) Xu, L.; Sevov, S. C. *J. Am. Chem. Soc.* **1999**, *121*, 9245. (b) Hauptmann, R.; Fässler, T. F. *Z. Anorg. Allg. Chem.* **2003**, *629*, 2266.
(14) Ugrinov, A.; Sevov, S. C. *J. Am. Chem. Soc.* **2002**, *124*, 10990. (b) Yong, L.; Hoffmann, S. D.; Fässler, T. F. *Z. Anorg. Allg. Chem.* **2005**, *631*, 1149.
(15) Ugrinov, A.; Sevov, S. C. *Inorg. Chem.* **2003**, *42*, 5789. (b) Yong, L.; Hoffmann, S. D.; Fässler, T. F. *Z. Anorg. Allg. Chem.* **2004**, *630*, 1977.
(16) (a) Downie, C.; Tang, Z.; Guloy, A. M. *Angew. Chem., Int. Ed.* **2000**, *39*, 338. (b) Downie, C.; Mao, J.-G.; Parmer, H., Guloy, A. M. *Inorg. Chem.* **2004**, *43*, 1992.
(17) Nienhaus, A.; Hauptmann R.; Fässler, T. F. *Angew. Chem., Int. Ed.* **2002**, *41*, 3213.
(18) Goicoechea, J. M.; Sevov, S. C. *Angew. Chem., Int. Ed.* **2006**, *45*, 5147.
(19) (a) Goicoechea, J. M.; Sevov, S. C. *J. Am. Chem. Soc.* **2004**, *126*, 6860. (b) Goicoechea, J. M.; Sevov, S. C. *Inorg. Chem.* **2005**, *44*, 2654.
(20) Hoch C.; Wendorff, M.; Röhr, C. *J. Alloys Compd.* **2003**, *361*, 206.
(21) von Schnering, H. G.; Baitinger, M.; Bolle, U.; Carrillo-Cabrera, W.; Curda, J.; Grin, Y.; Heinemann, F.; Llanos, J.; Peters, K.; Schmeding, A.; Somer, M. *Z. Anorg. Allg. Chem.* **1997**, *623*, 1037.
(22) Hoch, C.; Röhr, C. Wendroff, M. *Acta Crystallogr., Sect. C: Cryst. Struct. Commun.* **2002**, *58*, 45.

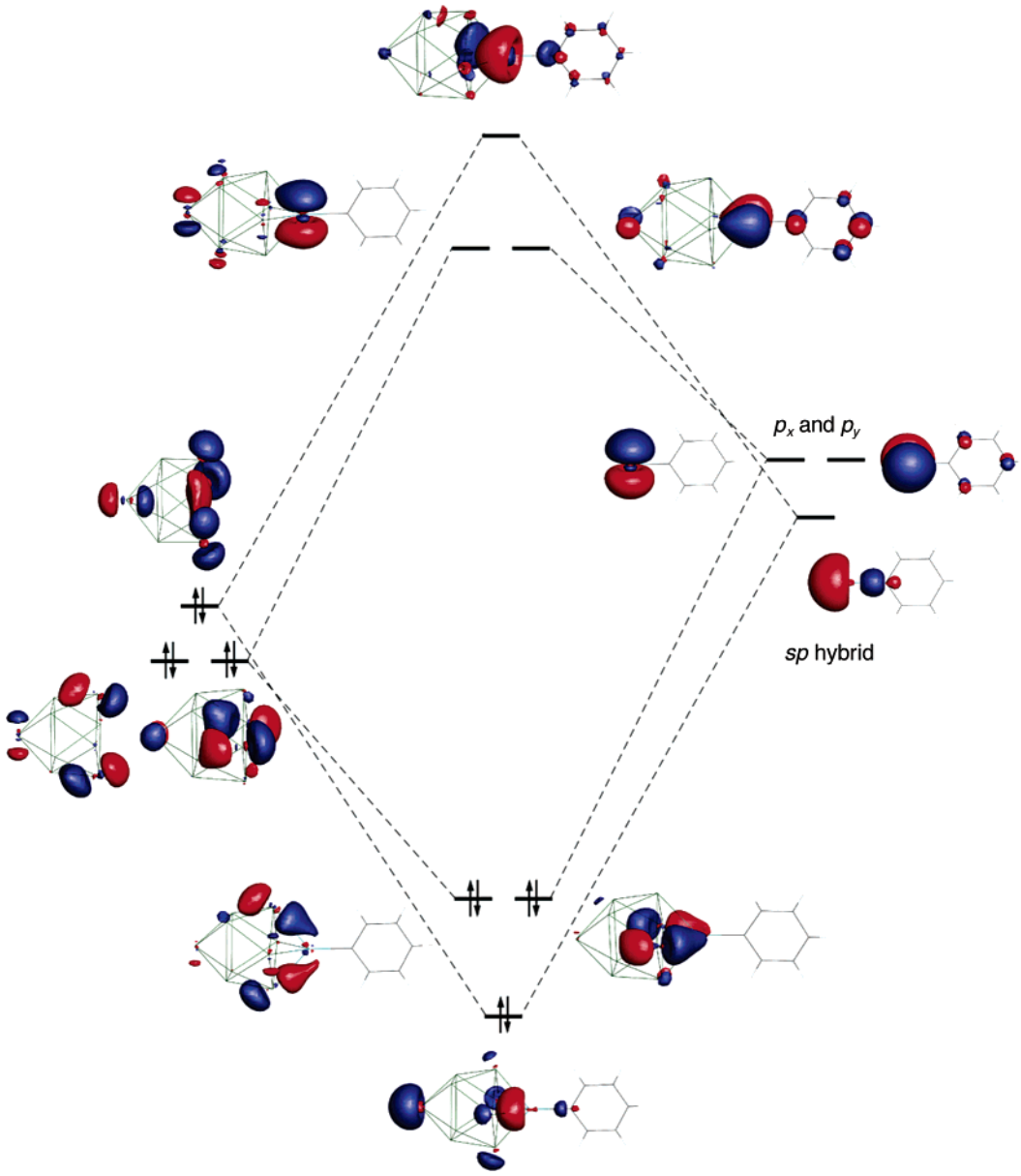

Figure 2. Fragment analysis of the interactions between the frontier orbitals of E_9 (left) and the ZnPh fragment (right) in the formation of $[E_9Zn\text{-}Ph]^{3-}$.

Ph]$^{3-}$, was crystallized in low yields from a pyridine solution of the product of the extraction of $K_{12}Si_{17}$ in liquid ammonia and $ZnPh_2$. As we have discussed previously for the specific case of the Ge_9 clusters, dissolution of the K_4Ge_9 Zintl phase in ethylenediamine yields an electron-rich solution where Ge_9^{4-} is in equilibrium with Ge_9^{3-}, Ge_9^{2-}, and, most likely, solvated electrons, i.e., $Ge_9^{4-} \rightleftharpoons Ge_9^{3-} + e^-(solv)$ and $Ge_9^{3-} \rightleftharpoons Ge_9^{2-} + e^-(solv)$.[11c] In all likelihood, these equilibria are also present for the other group 14 analogues judging by their similar reactivities. It should be pointed out that the presence of any positively charged transition metal fragments is extremely unlikely in such highly reducing solutions with solvated electrons. The reactions with $ZnPh_2$ were very "clean", producing the corresponding compounds in high yields, especially clusters **2**−**4**, and can be expressed with a balanced equation as $E_9^{4-} + ZnPh_2 \rightarrow [E_9Zn\text{-}Ph]^{3-} + Ph^-$. The phenyl anion is a very strong base and, as we have shown before, readily abstracts a proton from the ethylenediamine solvent to form benzene and amide.[11b]

Structure and Bonding. The shape of the $[E_9Zn\text{-}Ph]^{3-}$ clusters is that of a bicapped square antiprism where one of the capping vertexes is occupied by the zinc atom of the ZnPh fragment (Figure 1). The E−E distances are in the range 2.395(3)−2.689(3) Å for **1** (the quality of the crystals of **1** was poor, and the metric parameters are of low precision), 2.5427(7)−2.8377(8) Å for **2**, 2.9156(3)−3.2275(3) Å for **3**, and 3.0447(6)−3.4078(5) and 3.068(6)−3.3620(6) Å for the two crystallographically distinct clusters **4** in $[K(2,2,2\text{-crypt})]_6(\mathbf{4})_2 \cdot 2en \cdot tol$. They all compare nicely with previously reported distances for both naked and derivatized clusters. The Zn−E distances to the four atoms of the capped square are within very narrow ranges: 2.504(2)−2.531(3) Å for **1**, 2.5720(8)−2.5944(9) Å for **2**, 2.7397(4)−2.7867(4) Å for **3**, and 2.7883(13)−2.8411(12) and 2.8074(13)−2.8268(12) Å for **4**. Finally, the Zn−Ph distances 2.000(9), 1.994(5), 1.987(3), and 2.001(11) and 1.983(10) Å for Si, Ge, Sn, and the two Pb clusters, respectively, remain nearly identical from one cluster to the next, as expected. They compare well with Zn−Ph reported in the literature in

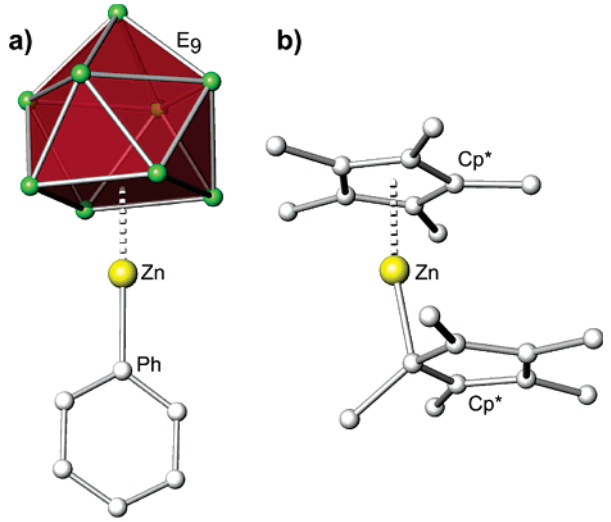

Figure 3. (a) $[E_9Zn\text{-}Ph]^{3-}$ and (b) (η^5-Cp*)Zn(η^1-Cp*).[26] In both species the Zn atoms exhibit a two-center−two-electron bond to an R group and interactions with the π-system of a six-electron donor.

compounds such as $[Zn(Ph)_3]^-$, with distances of 1.990(11), 2.006(9), and 2.026(11) Å,[23] and $[Zn(18\text{-crown-}6)]Ph_2$, with distances of 1.981(3) and 1.988(3) Å.[24] A full list of the distances within the clusters is given in Table 1.

The shape of the clusters, a bicapped square antiprism, is in line with the expected shape for a *closo*-cluster with 10 vertexes. According to Wade's electron-counting rules, such a cluster should have 22 ($2n + 2$, where n is the number of vertexes) electrons for cluster bonding, and, indeed, this is the case for $[E_9Zn\text{-}Ph]^{3-}$.[25] Each group 14 atom is a two-electron donor analogous to the B−H units of the well-known deltahedral borane clusters $B_nH_n^{m-}$. The remaining two electrons per atom form a lone pair and occupy an orbital that points radially outward of the cluster. Following the analogy with B−H, this pair of electrons corresponds to the pair of electrons of the hydrogen−boron bond. Similar analysis attributes one single electron to the Zn−R fragment; that is, one of the two valence electrons of the zinc atom is used for Zn−R bonding, while the second one is available for sharing within the cluster. Taking into account the 3− charge of the clusters, the number of cluster bonding electrons in $[E_9Zn\text{-}Ph]^{3-}$ can be calculated as $(9 \times 2) + 1 + 3 = 22$ electrons. There are clear similarities between these clusters and the previously reported clusters of $[E_9M(CO)_3]^{4-}$, where E = Sn, Pb and M = Cr, Mo, W.[2] All exhibit the same *closo*-geometry and have 22 electrons dedicated to cluster bonding. The difference in the charge between $[E_9Zn\text{-}Ph]^{3-}$ and $[E_9M(CO)_3]^{4-}$ arises as a result of the different numbers of electrons donated by the transition metal fragments, zero from $M(CO)_3$ and one from ZnPh.

Frontier orbital analysis reveals that the Zn atom in $[E_9Zn\text{-}Ph]^{3-}$ is sp hybridized, as expected, with one of the sp hybrid orbitals employed for *exo*-bonding to the phenyl ring. The remaining sp hybrid and the p_x and p_y orbitals overlap with E_9 orbitals and become part of the cluster molecular orbitals (Figure 2). The sp hybrid matches the symmetry of a filled E_9 orbital that is totally bonding within the open square and is made of atomic orbitals pointing toward the center of the square. The overlap between this cluster orbital and the sp hybrid at the ZnPh fragment indicates clearly σ bonding. The p_x and p_y orbitals of the fragment have their matches in the E_9 cluster as well. These cluster orbitals are degenerate and involve predominantly the p_π orbitals (out of phase) of pairs of opposite corners of the open square (Figure 2). They correspond to the well-known degenerate nonbonding π orbitals in square-planar cyclobutadiene. These two orbitals π-overlap with the two p orbitals of the ZnPh fragment. Therefore, the open square face of the cluster acts as a six-electron donor ligand equivalent to η^6-C_6H_6 or η^5-$C_5H_5^-$. A search of the literature revealed only one such direct analogue, namely, (η^5-Cp*)Zn(η^1-Cp*), shown in Figure 3 alongside the $[Ge_9Zn\text{-}Ph]^{3-}$ cluster.[26] There are several additional examples that feature (η^5-Cp*)Zn or (η^5-Cp)Zn moieties, but they are not bonded to carbon. They include $(Cp^*Zn)_2$,[27] $(Cp\text{-}Zn)_2CoCp(PPh_3)$,[28] and $(CpZn)NbH_2(Cp)_2$.[29] Similarly to benzene and the cyclopentadienyl anion, the open square face must be attractive to electrophilic species such as $M(CO)_3$ (M = Cr, Mo, W),[2] Ni(CO),[1] and ZnPh in order for them to complete their electron valence shells.

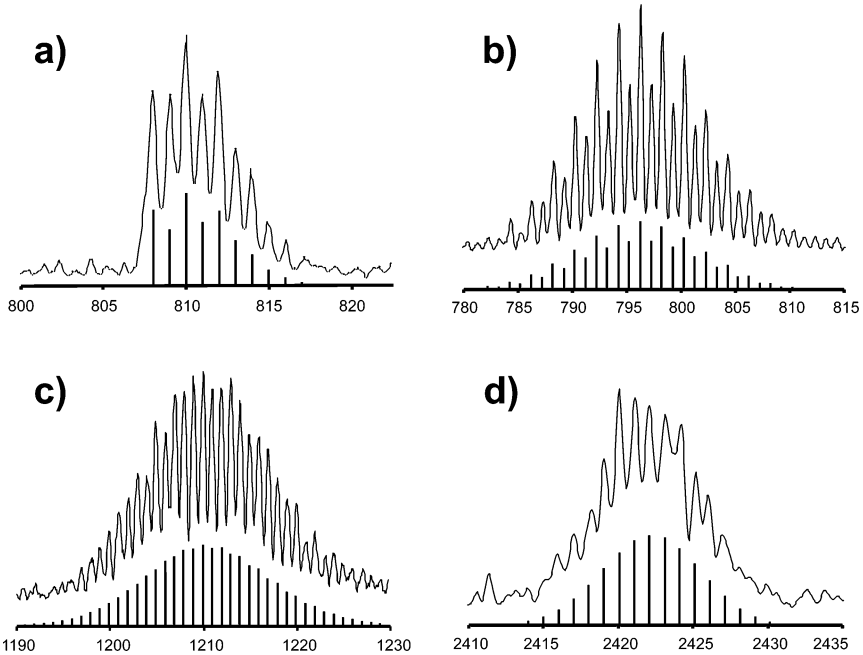

Figure 4. Selected negative ion mode electrospray mass spectrometric peaks corresponding to (a) $\{[K(2,2,2\text{-crypt})][Si_9Zn\text{-}Ph]\}^-$, (b) $[Ge_9Zn\text{-}Ph]^-$, (c) $[Sn_9Zn\text{-}Ph]^-$, and (d) $\{[K(2,2,2\text{-crypt})][Pb_9Zn\text{-}Ph]\}^-$. Shown under each peak is the calculated isotopic distribution.

Table 2. Selected Data Collection and Refinement Parameters for (K-crypt)$_3$1·2py, (K-crypt)$_3$2·2en·tol, (K-crypt)$_3$3·tol, and (K-crypt)$_6$4$_2$·2en·tol

	(K-crypt)$_3$**1**·2py	(K-crypt)$_3$**2**·2en•tol	(K-crypt)$_3$**3**·tol	(K-crypt)$_6$**4**$_2$·2en·tol
fw	1800.24	2254.89	2549.58	6720.23
space group, *Z*	$P\bar{1}$, 2	$P\bar{1}$, 2	$P2_1/n$, 4	$P\bar{1}$, 2
a (Å)	13.9464(5)	13.8684(4)	13.6322(4)	15.8267(4)
b (Å)	14.8743(6)	14.9256(4)	24.4665(8)	22.4460(7)
c (Å)	25.6457(9)	25.9765(7)	28.0370(9)	27.5057(8)
α (deg)	76.954(2)	76.627(2)		87.793(2)
β (deg)	84.974(2)	84.302(2)	94.295(2)	74.942(2)
γ (deg)	67.988(2)	68.919(2)		89.428(2)
V (Å^3)	4804.9(3)	4880.3(2)	9325.0(5)	9428.8(5)
ρ_{calc} (g·cm^{-3})	1.244	1.534	1.816	2.367
radiation, *λ* (Å), temp (K)		Mo Kα, 0.71073, 100		
μ (cm^{-1})	0.559	3.160	2.812	16.447
R1/wR2,[a] $I \geq 2\sigma_I$ (%)	8.53/25.21	4.88/14.34	3.71/6.58	4.16/10.11
R1/wR2,[a] all data (%)	15.65/29.39	6.47/15.49	6.03/7.54	6.57/10.90

[a] $R1 = [\sum||F_o| - |F_c||]/\sum|F_o|$; $wR2 = \{[\sum w[(F_o)^2 - (F_c)^2]^2]/[\sum w(F_o^2)^2]\}^{1/2}$; $w = [\sigma^2(F_o)^2 + (AP)^2 + BP]^{-1}$, where $P = [(F_o)^2 + 2(F_c)^2]/3$ and the *A* and *B* values are 0.1798 and 0.00 for (K-crypt)$_3$**1**·2py, 0.0872 and 17.07 for (K-crypt)$_3$**2**·2en·tol, 0.0102 and 34.85 for (K-crypt)$_3$**3**·tol, and 0.0619 and 0.00 for (K-crypt)$_6$**4**$_2$·2en·tol.

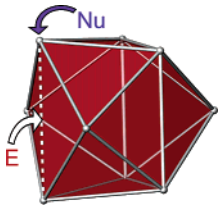

Figure 5. Representation of the sites for electrophilic (E) substitution and nucleophilic (Nu) attack in a Ge_9^{n-} cluster. The dotted line represents an elongated edge of the tricapped trigonal prism (vertical pseudo-three-fold axis). This shape resembles also a monocapped square antiprism where the open square face is the site for the electrophilic substitution.

DFT calculations revealed a similar picture for all four [E$_9$-Zn-Ph]$^{3-}$ clusters. The two semidegenerate π^* orbitals of the phenyl ring are always found in the gap between the HOMO and the first cluster-based LUMO (LUMO+2). The same effect was observed previously for [Ni@Ge$_9$NiCCPh]$^{3-}$. The calculated HOMO−LUMO gaps are very similar for the four clusters: 2.82, 2.64, 2.82, and 2.56 eV for Si, Ge, Sn, and Pb, respectively. On the other hand, the gaps between the cluster-based orbitals, i.e., HOMO-to-LUMO+2, decrease upon going down the group: 4.07, 3.87, 3.15, and 2.93 eV for Si, Ge, Sn, and Pb, respectively. These gaps clearly indicate good stability for all four cluster species and suggest a relative inertness toward oxidation or reduction.

Characterization in Solution. All four compounds were found to be soluble in DMF, and their electrospray mass spectra were recorded from such solutions in both the negative and positive ion modes. Due to the multiple isotopes of K, Zn, Si, Ge, Sn, and Pb, all peaks appear as very distinctive mass envelopes allowing for their unequivocal assignments on account of the characteristic isotopic fingerprints. As we have previously observed for the mass spectra of other anionic Zintl clusters in the negative ion mode, they appear with reduced charges due to cluster oxidation during the electrospray process and often are ion paired with [K(2,2,2-crypt)]$^+$. Thus, the negative ion mode spectra of [K(2,2,2-crypt)]$_3$**1**·2py, [K(2,2,2-crypt)]$_3$**2**·2en·tol, [K(2,2,2-crypt)]$_3$**3**·tol, and [K(2,2,2-crypt)]$_3$**4**$_2$·2en·tol revealed peaks corresponding to the [E$_9$Zn-Ph]$^{3-}$ clusters with a single negative charge, i.e., [E$_9$Zn-Ph]$^-$ at *m*/*z* values of 395.1, 796.3, 1210.0, and 2006.9 for Si, Ge, Sn, and Pb, respectively (Figure 4). Similarly, these spectra also revealed the ion-paired species {[K(2,2,2-crypt)][E$_9$Zn-Ph]}$^-$ at *m*/*z* 810.1, 1212.4, 1626.2, and 2422.1 for Si, Ge, Sn, and Pb, respectively (Figure 4). In addition, there are also very weak peaks corresponding to the extensively ion-paired species {[K(2,2,2-crypt)]$_2$[E$_9$Zn-Ph]}$^-$ for all four cluster compounds, as well as peaks arising from cluster fragmentation, namely, [E$_9$]$^-$ arising from the loss of the ZnPh moiety. The positive ion mode spectra also showed evidence of the clusters revealing peaks corresponding to the extensively ion-paired species {[K(2,2,2-crypt)]$_4$[E$_9$Zn-Ph]}$^+$ for E = Ge, Sn, Pb and {[K(2,2,2-crypt)]$_3$[E$_9$Zn-Ph]}$^+$ for E = Si, Ge, Pb.

In addition to the characterization by mass spectroscopy, clusters **2**−**4** were characterized in solution also by $^{13}C\{^1H\}$ NMR (the low yield of **1** prevented its characterization by NMR). The spectra show four clear resonances corresponding to the four distinct carbon environments of the phenyl rings in [E$_9$Zn-Ph]$^{3-}$ with no presence of any additional signals in the aromatic region, and this indicates that the clusters remain intact in solution. Furthermore, it also shows either that there is no fluxionality of the Zn−Ph vertex, i.e., the fragment does not occupy different positions in the cluster, or that any fluxionality is too fast at room temperature to be registered on the NMR time scale. The spectra of the different clusters **2**, **3**, and **4** do not differ greatly from one to another, as is to be expected of such chemically similar systems. The most notable difference is in the resonance shift of the *ipso*-carbon, which is most strongly affected by the different cluster atoms.

General Remarks. As already discussed, main group anionic nucleophiles invariably attack one of the vertexes of the triangular faces of the tricapped trigonal prism, as pictured in Figure 5. The reason for this is that the LUMO of E_9^{2-} is made predominantly of the p_z orbitals (*z* is vertical in Figure 5) of these six atoms. This molecular orbital protrudes outside the cluster as an extension of the vertical trigonal prismatic edges and is also relatively low in energy. This makes it readily available for bonding interactions with nucleophiles, and this is why the *exo*-bonds to the main group nucleophilic substituents are always extensions of the vertical prismatic edges. The

(23) Krieger, M.; Geiseler, G.; Harms, K.; Merle, J.; Massa, W.; Dehnicke, K. *Z. Anorg. Allg. Chem.* **1998**, *624*, 1387.
(24) Fabicon, R. M.; Parvez, M.; Richey, H. G. *Organometallics* **1999**, *18*, 5163.
(25) Wade, K. J. *Adv. Inorg. Chem. Radiochem.* **1976**, *18*, 1.
(26) Fischer, B.; Wijkens, P.; Boersma, J.; van Koten, G.; Smeets, W. J. J.; Spek, A. L.; Budzelaar, P. H. M. *J. Organomet. Chem.* **1989**, *375*, 223.
(27) Resa, I.; Carmona, E.; Gutierrez-Puebla, E.; Monge, A. *Science* **2004**, *305*, 1136.
(28) Budzelaar, P. H. M.; Boersma, J.; van der Kerk, G. J. M.; Spek, A. L.; Duisenberg, A. J. M. *Inorg. Chem.* **1982**, *21*, 3777.
(29) Budzelaar, P. H. M.; den Haan, K. H.; Boersma, J.; van der Kerk, G. J. M.; Spek, A. L. *Organometallics* **1984**, *3*, 156.

electrophilic species such as the isolobal $M(CO)_3$ (M = Cr, Mo, W) and Ni(CO) fragments, on the other hand, appear to have a preference for capping the open square face of the E_9 clusters (Figure 5). As already discussed, at this position they can find three available cluster orbitals with six electrons. Therefore, according to the site preference of the ZnPh fragment in the $[E_9Zn\text{-}Ph]^{3-}$ clusters, it belongs to the group of electrophiles and behaves as an electron-poor transition metal fragment and not as a main group nucleophile.

The four clusters reported here represent a complete family of ZnPh-functionalized nine-atom clusters of group 14 except carbon. They are the first species in which the capping fragment donates electrons to the pool of cluster bonding electrons. As such, these capped clusters open up a wealth of new possibilities in the field of Zintl cluster chemistry as we look beyond the metals of groups 6 and 10. In addition, from a coordination chemist's viewpoint these four novel species are also of interest as they are comparatively similar to the numerous organometallic species containing cyclic polyene ligands such as cyclopentadiene, which have been the subject of great interest throughout the history of organometallic chemistry. In more than one way, the nine-atom Zintl anions of Si through Pb represent heavier and more reduced analogues of these well-studied hydrocarbon ligands. Similar analogies can be drawn with numerous metallacarborane clusters such as $(1,2\text{-}C_2B_9H_{11})Co(Cp)$, where 11-vertex carborane systems act as six-electron donors to the transition metals, making them electronically saturated 18-electron systems.[30] As in the $[E_9Zn\text{-}Ph]^{3-}$ clusters (E = Si, Ge, Sn, and Pb), the metal atoms also fully partake in cluster bonding. While the use of main group Zintl clusters as ligands in coordination chemistry may still be far from commonplace, these new species prove that such compounds can be readily synthesized and may be the subject of study, as many transition metal cyclopentadienyl species have been before them.

Experimental Section

General Data. All manipulations were carried out under inert atmosphere using standard Schlenk-line and/or glovebox techniques. Ethylenediamine (Acros, 99%) was distilled over sodium metal and stored in a gastight ampule under nitrogen. Anhydrous ammonia (Matheson) was used as received. Zintl precursors $K_{12}Si_{17}$ and K_4E_9 (E = Ge, Sn, Pb) were synthesized from stoichiometric mixtures of the elements (K: 99+%, Strem; Si: 99.9999%, Ge 99.999% Sn: 99.999%, Pb: 99.9998%, Alfa-Aesar) heated at 900 °C over 2 days in sealed niobium containers jacketed in evacuated fused-silica ampules according to previously reported synthetic procedures.[20−22] 2,2,2-crypt (Acros, 98%) and $Zn(C_6H_5)_2$ (Strem, 99%) were used as received after carefully drying them under vacuum. Electrospray mass spectra were recorded from DMF solutions (10−20 μM) on a Micromass Quattro-LC triple quadrupole mass spectrometer (100 °C source temperature, 125 °C desolvation temperature, 2.5 kV capillary voltage, and 30 V cone voltage).

$^{13}C\{^1H\}$ and ^1H NMR spectra of **2**−**4** were recorded in ethylenediamine solutions using a Varian UNITYplus 300 MHz spectrometer and referenced to an internal capillary containing TMS (10% in CD_3OD).

$[K(2,2,2\text{-crypt})]_3[Si_9Zn(C_6H_5)]\cdot 2py$. $K_{12}Si_{17}$ (97 mg, 0.103 mmol) and 2,2,2-crypt (218 mg, 0.579 mmol) were weighed out into a Schlenk tube inside a glovebox, and the reaction vessel was subsequently transferred to a Schenk line where approximately 5 mL of $NH_3(l)$ was condensed over the solids at −70 °C. The resulting dark red solution was allowed to stir for 2 h, after which the NH_3 was allowed to evaporate off and the solid dried under vacuum. The solid, a mixture of Si_9^{3-} and Si_9^{2-},[19] was transferred to a glovebox, where it was redissolved in pyridine (3 mL) and reacted with $Zn(C_6H_5)_2$ (50 mg, 228 mmol). The reaction mixture was stirred for 1 h and filtered, and the filtrate was layered with toluene to allow for crystallization. Very thin yellow plates of $[K(2,2,2\text{-crypt})]_3[Si_9Zn(C_6H_5)]\cdot 2py$ were obtained alongside a brownish oil of unknown composition after several days. ES- MS: *m/z* 810.1 $\{(K\text{-crypt})[Si_9Zn(C_6H_5)]\}^-$, 395.1 $[Si_9Zn(C_6H_5)]^-$.

$[K(2,2,2\text{-crypt})]_3[Ge_9Zn(C_6H_5)]\cdot 2en\bullet tol$. K_4Ge_9 (102 mg, 0.126 mmol) and 2,2,2-crypt (169 mg, 0.448 mmol) were dissolved in ethylenediamine (3 mL) in a test tube inside a glovebox and allowed to stir for approximately 5 min before the addition of $Zn(C_6H_5)_2$ (64 mg, 0.232 mmol). The reaction mixture was stirred for 1 h, after which the resulting bright orange-red solution was filtered and the filtrate layered with toluene to allow for crystallization. Large bright orange block-shaped crystals suitable for single-crystal X-ray diffraction were obtained after 2 days (64% crystalline yield). $^{13}C\{^1H\}$ NMR (en, CD_3OD/TMS capillary): δ 180.1 (s, *i*-C_6H_5), 138.4 (s, *o*-C_6H_5), 126.4 (s, *m*-C_6H_5), 123.2 (s, *p*-C_6H_5), 71.5 (s, 2,2,2-crypt), 68.6 (s, 2,2,2-crypt), 54.9 (s, 2,2,2-crypt). ES- MS: *m/z* 1212.4 $\{(K\text{-crypt})[Ge_9Zn(C_6H_5)]\}^-$, 1796.3 $[Ge_9Zn(C_6H_5)]^-$.

$[K(2,2,2\text{-crypt})]_3[Sn_9Zn(C_6H_5)]\cdot tol$. K_4Sn_9 (123 mg, 0.100 mmol) and 2,2,2-crypt (155 mg, 0.412 mmol) were dissolved in ethylenediamine (3 mL) in a test tube inside a glovebox and allowed to stir for approximately 5 min before the addition of $Zn(C_6H_5)_2$ (27 mg, 0.123 mmol). The reaction mixture was stirred for 1 h, after which the resulting dark reddish-black solution was filtered and the filtrate layered with toluene to allow for crystallization. Large dark red-black brick-shaped crystals suitable for single-crystal X-ray diffraction were obtained after 2 days (30% crystalline yield). $^{13}C\{^1H\}$ NMR (DMF, CD_3OD/TMS capillary): δ 166.7 (s, *i*-C_6H_5), 136.5 (s, *o*-C_6H_5), 127.0 (s, *m*-C_6H_5), 123.3 (s, *p*-C_6H_5), 71.5 (s, 2,2,2-crypt), 68.7 (s, 2,2,2-crypt), 55.0 (s, 2,2,2-crypt). ES- MS: *m/z* 1626.2 $\{(K\text{-crypt})[Sn_9Zn(C_6H_5)]\}^-$, 1210.0 $[Sn_9Zn(C_6H_5)]^-$.

$[K(2,2,2\text{-crypt})]_6[Pb_9Zn(C_6H_5)]_2\cdot 2en\cdot tol$. K_4Pb_9 (200 mg, 0.10 mmol) and 2,2,2-crypt (160 mg, 0.43 mmol) were dissolved in ethylenediamine (3 mL) in a test tube inside a glovebox and allowed to stir for approximately 5 min before the addition of $Zn(C_6H_5)_2$ (28 mg, 0.13 mmol). The reaction mixture was stirred for 1 h, after which the resulting dark reddish-black solution was filtered and the filtrate layered with toluene to allow for crystallization. Dark red-black brick-shaped crystals suitable for single-crystal X-ray diffraction were obtained after 2 days (68% crystalline yield). $^{13}C\{^1H\}$ NMR (DMF, CD_3OD/TMS capillary): δ 164.5 (s, *i*-C_6H_5), 131.8 (s, *o*-C_6H_5), 128.1 (s, *m*-C_6H_5), 122.5 (s, *p*-C_6H_5), 71.9 (s, 2,2,2-crypt), 69.1 (s, 2,2,2-crypt), 55.3 (s, 2,2,2-crypt). ES- MS: *m/z* 2422.1 $\{(K\text{-crypt})[Pb_9Zn(C_6H_5)]\}^-$, 2006.9 $[Pb_9Zn(C_6H_5)]^-$.

Crystallographic Studies. Single-crystal X-ray diffraction data sets were collected on a Bruker APEX II diffractometer with a CCD area detector at 100 K with Mo Kα radiation. The crystals were selected under Paratone-N oil, mounted on fibers, and positioned in the cold stream of the diffractometer. The structures were solved by direct methods and refined on F^2 using the SHELXTL V6.21 package.[31] Details of the four data collections reported in this paper are provided in Table 2. All examined crystals of **1** were of poor quality, and this resulted in structure determination of lower precision.

Computational Methods. All calculations were performed on the clusters using atomic positions as elucidated by single-crystal X-ray diffraction data. Single-point DFT calculations were carried out

(30) Hawthorne, M. F. *J. Orgamomet. Chem.* **1975**, *100*, 97.
(31) Scheldrick, G. M. *SHELXTL*, version 6.21; Bruker-Nonius AXS: Madison, WI, 2001.
(32) Becke, A. D. *J. Chem. Phys.* **1993**, *98*, 5648.
(33) (a) Lee, C.; Yang, W.; Parr, R. G. *Phys. Rev.* **1988**, *B37*, 785. (b) Miehlich, B.; Savin, A.; Stoll, H.; Preuss, H. *Chem. Phys. Lett.* **1989**, *157*, 200.

employing the Becke three-parameter hybrid functional with Lee−Yang−Parr correlation (B3LYP) in conjunction with the LanL2DZ basis set[32−34] and were executed with the Gaussian 98 package, revision A.11.3,[35] on Notre Dame's "Bunch-o-Boxes" Beowulf cluster. Frontier orbital analyses on the clusters were performed with the Jimp 2 program, version 0.089, and the orbitals represented with MOPLOT2.[36]

Acknowledgment. We thank the National Science Foundation for the financial support of this research (CHE-0446131) and for the purchase of a Bruker APEX II diffractometer (CHE-0443233) and the "Bunch-o-Boxes" cluster (DMR-0079647). We also acknowledge Dr. Bill Boggess for his assistance with all mass spectrometric experiments.

Supporting Information Available: X-ray crystallographic file in CIF format (four structures), drawings of the four cluster species with anisotropic displacement ellipsoids, and complete ref 35. This material is available free of charge via the Internet at http://pubs.acs.org.

OM060481G

(34) (a) Hay, P. J.; Wadt, W. R. *J. Chem. Phys.* **1985**, *82*, 270. (b) Wadt, W. R.; Hay, P. J. *J. Chem. Phys.* **1985**, *82*, 284. (c) Hay, P. J.; Wadt, W. R. *J. Chem. Phys.* **1985**, *82*, 299.

(35) Frisch, M. J.; et al. *Gaussian98*, revision A.11.3; Gaussian, Inc.: Pittsburgh, PA, 2002.

(36) (a) Manson, J. M. B.; Webster, C. E.; Hall, M. B. *Jimp 2* Version 0.089 (January 31 2006); Department of Chemistry, Texas A&M University: College Station, TX 77842 (http://www.chem.tamu.edu/jimp2/). (b) Hall, M. B.; Fenske, R. F. *Inorg. Chem.* **1972**, *11*, 768. (c) Lichtenberger, D. L. *MOPLOT2*, for orbital and density plots from linear combinations of Slater or Gaussian type orbitals, Version 2.0, June 1993; Department of Chemistry, University of Arizona: Tuscon, AZ 85721, 1993.